

## WORK HARDENING ANISOTROPY GENERATED BY CUBE TEXTURE IN COMMERCIAL PURITY ALUMINIUM

B.P. Wynne\*, P.Cizek\*, C.H.J. Davies\*, M. Kubota\* and B.A. Parker\*\*

\* Department of Materials Engineering, Monash University, Clayton, Victoria 3168, Australia

\*\* Faculty of Engineering, University of Wollongong, Wollongong, NSW 2522, Australia

**Abstract** The mechanical anisotropy generated by a strong cube texture in commercial purity AA1050 aluminium alloy has been studied as a function of temperature. The investigation has shown that, under conditions of athermal hardening, tensile directions parallel and perpendicular to the rolling direction work harden at a greater rate than tensile directions at 22° and 45° to the rolling direction. Whereas, in the dynamic recovery deformation regime the situation is reversed.

**Keywords:** *Mechanical Anisotropy, Cube Texture, Work Hardening*

### 1. Introduction

The mechanical anisotropy generated by preferred crystallographic orientation of grains (texture) is well-known to be important in determining the formability of sheet metal. The most widely received models [1,2] to predict the anisotropy are based purely on geometrical restrictions of crystallographic slip and, thus, predict the same level of anisotropy regardless of temperature and strain rate. The intention of the present paper is to investigate whether mechanical anisotropy generated by texture is based entirely on geometrical restrictions of slip or can be influenced by deformation temperature.

### 2. Experimental Material and Method

A commercial purity aluminium alloy AA1050 sheet, 1.2 mm thick and received in the full-hard condition, was the material used for the study. Tensile samples, with a gauge length of 60 mm and width of 12.5 mm, were cut at angles of 0°, 22°, 45°, and 90° to the rolling direction (RD). The samples were annealed at a temperature of 573 K for 1 h. in an air circulating furnace and air cooled. The recrystallised grain size was approximately 30 µm and the grains were equiaxed.

Mechanical properties were measured using an INSTRON 4505 machine with displacement measured using an LVDT. Tensile tests were carried out at a strain rate of  $10^{-4}$  s<sup>-1</sup> and at temperatures of 77 K and 298 K. Work hardening rates,  $d\sigma/d\varepsilon$ , were determined by fitting a least squares polynomial of degree 1 to three successive data points (strain range 0.0003). The resulting slope of the straight line was then assumed to be the work hardening rate.

Texture measurements were made on the as-recrystallised sample and on deformed tensile samples at strains of 0.1 to 0.4. For the cases of the 0° and 90° to RD directions deformed at 298 K, texture measurements were only done to a strain of 0.3 due to the onset of necking occurring at strains less than 0.4. Incomplete {111}, {200}, and {220} pole figures were collected using a PHILIPS 1050 x-ray goniometer and corrected for background and defocusing. Pole figure construction and Orientation Distribution Function (ODF) analysis were performed using the POPLA software [3]. Using POPLA, the mean Taylor factor,  $\bar{M}$ , was calculated.

### 3. Experimental Results

Fig. 1 shows the recalculated {200} pole figure of the as-recrystallised sample. The material has a well developed cube (001)[100] texture. The corresponding ODF showed a small drift of orientations towards (011)[100] and a small amount of retained rolling texture, however, the material can essentially be considered a polycrystal with an orientation distribution approximating a single orientation, (001)[100].

The stress-strain curves for the directions tested, as a function of temperature, are shown in Fig. 2. The curves clearly indicate that the presence of the texture leads to flow properties which are strongly dependent on orientation. Also highlighted is the strength of the cube texture, with the crystallographically similar directions  $0^\circ$  and  $90^\circ$  having the most alike flow properties. Furthermore, the anisotropy appears to be dependent on the temperature of testing. At 298 K (Fig. 2a), both the  $0^\circ$  and  $90^\circ$  directions have a higher level of flow stress until a strain of approximately 0.06, whereupon the  $22^\circ$  and  $45^\circ$  directions begin to have a greater flow stress. This behaviour corresponds with the work of Li and Bate [4] for a similar alloy (AA1100) with similar starting texture.

However, the development of flow stress anisotropy for material tested at 77 K differs from that of 298 K. At 77 K, the strain for which the  $0^\circ$  direction has a higher flow stress is much greater, with the  $45^\circ$  and  $22^\circ$  directions not having higher flow stresses until strains of approximately 0.28 and 0.32 respectively.

Incomplete  $\{200\}$  experimental pole figures for the aluminium alloy deformed at  $T = 298$  K to a strain of 0.3 for all testing directions are shown in Fig. 3. For the  $0^\circ$  and  $90^\circ$  directions, there appears to be no significant change in the cube texture. Whereas, for the  $22^\circ$  and  $45^\circ$  directions, there is a splitting of the rotated cube texture component into two approximately equal components rotated about an axis close to the tensile specimen's transverse direction. For the  $45^\circ$  direction, the axis of rotation appears to be exactly the transverse direction, whereas for the  $22^\circ$  direction this axis appears to be at a small angle to the transverse direction. Similar behaviour and similar levels of texture intensity, as a function of strain, were also obtained for the material deformed at 77 K [5]. Fig. 4 shows an example of the texture evolution of the  $45^\circ$  direction as a function of temperature. This plot shows the texture intensity from the ODFs of material rotated about the transverse axis during deformation to a strain of 0.3. There is no significant variation of the orientation distribution as a function of rotation about the transverse direction for the two testing conditions. However, at 77 K, there appears to be more material with orientations with less rotation about the transverse direction, *ie* there appears to be a slight lag for deformation at 77 K compared to material deformed at 298 K for the same level of strain.

Table 1 displays the calculated mean Taylor factors,  $\bar{M}$ , for the as-recrystallised material and for material deformed at both testing temperatures to a strain of 0.3. For the  $0^\circ$ ,  $22^\circ$  and  $90^\circ$  testing directions to RD, the average Taylor factor remained virtually constant compared to the as-recrystallised material. For the  $45^\circ$  direction, there is an increase of approximately 0.1 for both testing temperatures.

The work hardening behaviour of the material deformed at 77 K for the  $0^\circ$ ,  $22^\circ$  and  $45^\circ$  directions to RD is shown in Fig. 5a in the form of a  $\sigma \delta\sigma/\delta\epsilon$  vs.  $\sigma$  plot. This type of plot has been shown to be very good at identifying different regions of the work hardening curve for polycrystal deformation [6]. The hardening behaviour appears to consist of two stages. Initially, all directions exhibit linearly increasing values of  $\sigma\theta$  with  $\sigma$ , which is subsequently followed by a decreasing rate of hardening. This corresponds to athermal type hardening behaviour, followed by dynamic recovery which is temperature sensitive. It is clear from Fig. 5a that, under conditions of athermal

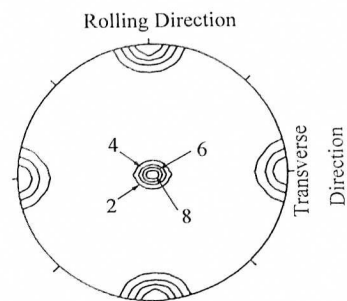


Fig. 1.  $\{200\}$  recalculated pole figure of the as-recrystallised sample. Contours represent multiples of random density.

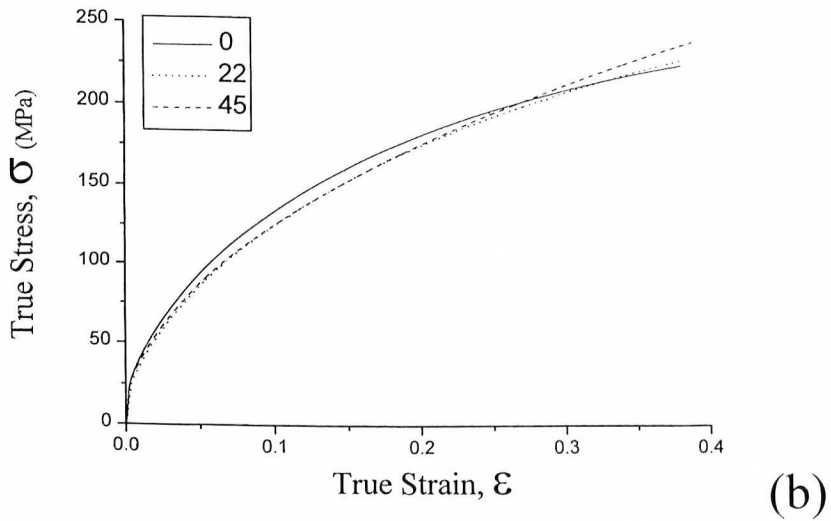
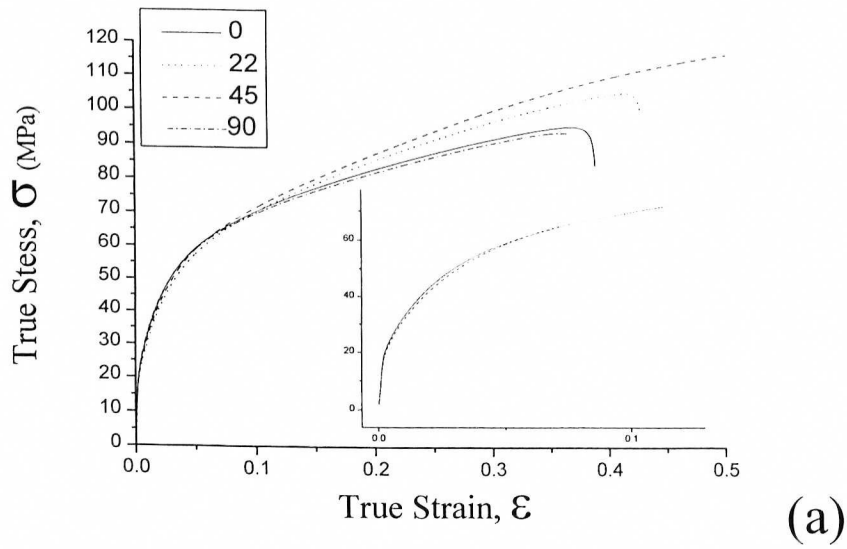


Fig. 2. Tensile stress/strain curves: (a) 298 K; insert displays small strain range and, (b) 77 K. For clarity of presentation, the stress-strain curve for the 90° sample is shown only for 298 K.

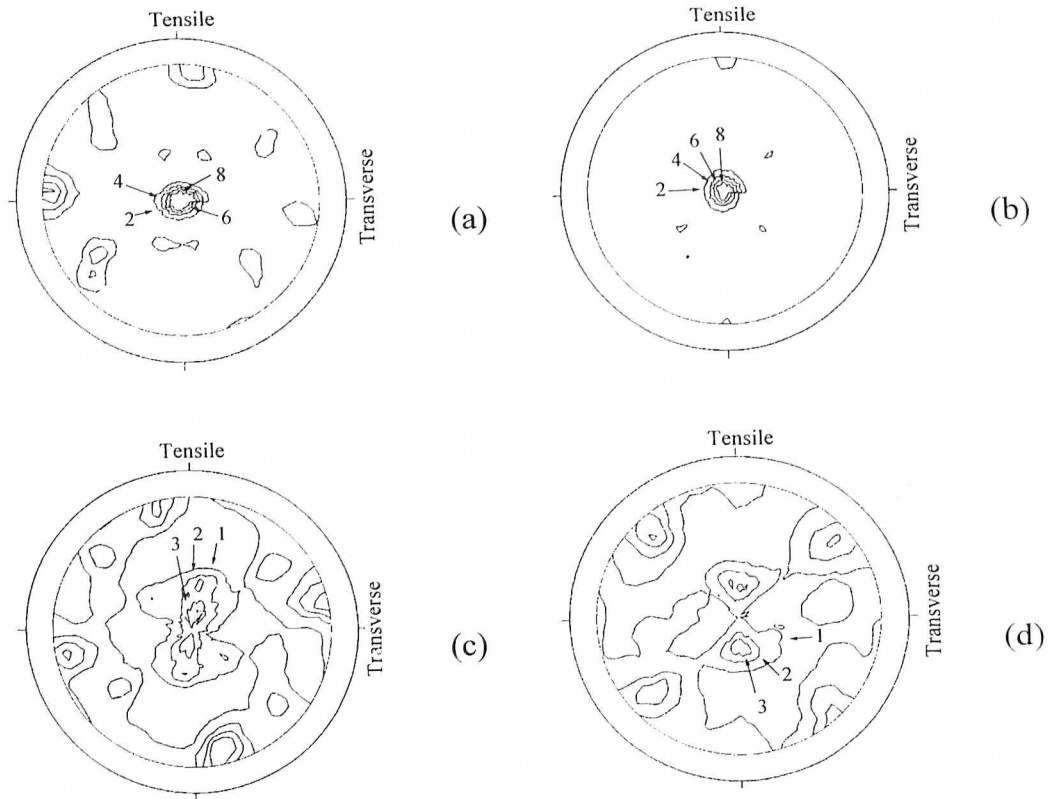


Fig. 3. Experimental  $\{200\}$  pole figures for AA1050 deformed to a strain of 0.3 at 298 K (a)  $0^\circ$  to RD, (b)  $90^\circ$  to RD, (c)  $22^\circ$  to RD and (d)  $45^\circ$  to RD. Contours represent multiples of random density.

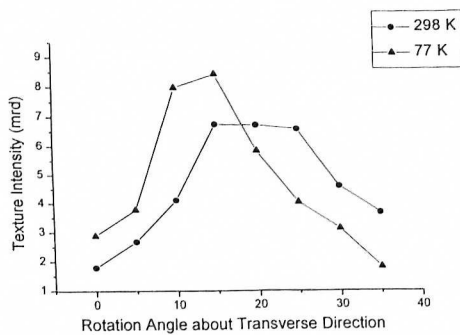


Fig. 4. Orientation intensity of material rotated about the transverse direction to a strain of 0.3 for the specimens deformed at  $45^\circ$  to RD. (mrd = multiples of random density)

Table 1. Mean Taylor factors,  $\bar{M}$ , for uniaxial tension calculated from harmonic texture coefficients

Angle to RD	As - Annealed	Testing Temperature	
		298 K $\epsilon = 0.3$	77 K $\epsilon = 0.3$
$0^\circ$	2.89	2.89	2.91
$22^\circ$	3.00	2.99	2.97
$45^\circ$	3.09	3.18	3.18
$90^\circ$	2.92	2.84	2.91

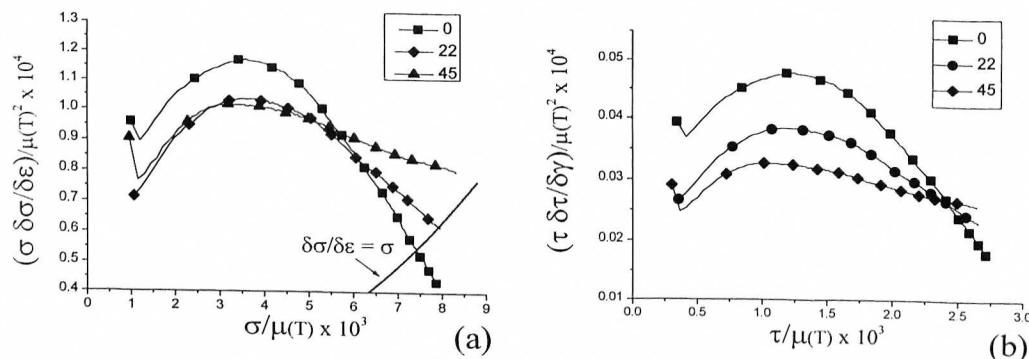


Fig. 5. (a)  $\sigma \delta\sigma/\delta\epsilon$  vs.  $\sigma$  plot of AA1050 deformed at 77 K for testing directions of  $0^\circ$ ,  $45^\circ$  and  $90^\circ$  to the RD, and (b) the equivalent  $\tau \delta\tau/\delta\gamma$  vs.  $\tau$  texture compensated plot.  $\mu(T)$  is the temperature dependent shear modulus.

hardening, the  $0^\circ$  direction has enhanced work hardening compared to the other two directions. Conversely, in the dynamic recovery regime, there is enhanced recovery in the  $0^\circ$  direction in comparison to the  $22^\circ$  and  $45^\circ$  directions. To determine if this variation in angular properties is due to a variation in texture, a  $\tau \delta\tau/\delta\gamma$  vs.  $\tau$  plot is given in Fig. 5b. The values for Fig. 5b were determined using the equation  $\sigma = \bar{M}\tau$  and the values of  $\bar{M}$  calculated from the texture measurements. This figure clearly indicates the variation described above. The equivalent diagrams for the material deformed at 298 K show a similar behaviour, except the curves are shifted to the left such that there is less athermal type hardening.

#### 4. Discussion

The results of the present work show that the flow stress anisotropy, generated by a strong cube texture in AA1050, is influenced by the deformation temperature. Most importantly, it appears that a significant component of the anisotropy is generated by an orientation dependence of the work hardening behaviour, *ie* the anisotropy depends on the stage of work hardening. Furthermore, the greater level of work hardening in the athermal stage and subsequent enhanced dynamic recovery for the  $0^\circ$  and  $90^\circ$  directions corresponded to texture stability. On the other hand, lower levels of athermal hardening and reduced dynamic recovery corresponding to the  $22^\circ$  and  $45^\circ$  directions correlated to textures which split during tensile straining into two orientation groups, that rotated in opposite directions about an axis close to the transverse direction. For the  $0^\circ$  and  $90^\circ$  directions, the texture stability means that the flow behaviour is totally dependent on the change in slip resistance,  $\delta\tau$ . For the  $22^\circ$  and  $45^\circ$  directions, there is a change in the texture with strain which may lead to a temperature dependence of the evolution of the geometrical factor between the resistance to slip,  $\tau$ , and the applied stress,  $\sigma$ , (*eg* the Taylor factor where  $\sigma = \bar{M}\tau$ ) on top of the change in  $\tau$ . However, there only appears to be minor differences between texture evolution for the two testing temperatures (Fig. 4) which, in turn, do not seem to have a large influence on the average geometric factor (Table 1). This temperature insensitivity of texture development also indicates that the active slip systems are independent of the stage of hardening and, therefore, must be a function of the geometrical requirements of deformation. Hence, it appears that the variation in anisotropy with temperature derives from a variation in the mutual interactions of the active slip systems for the different testing directions at different stages of work hardening.

Apart from the cube texture remaining stable for the  $0^\circ$  and  $90^\circ$  directions to RD, it has been noted [5] that the ratio of the width and thickness strain for these two directions was close to unity.

The slip systems operative to fulfill both the above conditions would have to be  $-a_2$ ,  $a_3$ ,  $b_2$ ,  $-b_3$ ,  $c_2$ ,  $-c_3$ ,  $-d_2$  and  $d_3$  in the nomenclature of Bishop and Hill [7]. For the  $45^\circ$  direction to RD, the strain in the width direction was close to zero. This corresponds to work shown previously [4,8], indicating that the slip systems operating in any one volume element are the coplanar systems  $a_1$  and  $-a_2$  or  $b_1$  and  $-b_2$ . The  $22^\circ$  direction also has a width strain close to zero. However, the prediction of the corresponding active slip systems is not simple but it could be envisaged that, similarly to the  $45^\circ$  direction, there are two groups of active systems rotating the material in opposite directions, but with maybe 3 active systems in each group.

The above discussion has given an insight into the observed temperature sensitivity of the flow anisotropy observed. With 8 active slip systems within each deforming volume element for the  $0^\circ$  and  $90^\circ$  directions to RD, the probability of dislocation interaction is very high leading to high rates of athermal hardening. Conversely, under dynamic recovery deformation conditions, the 8 active slip systems offer a high probability of cross-slip occurring (*ie* there are 4 active cross-slip system pairs:  $-a_2, -d_2$ ;  $b_2, c_2$ ;  $-c_3, d_3$ ;  $a_3, -b_3$  [5]) which would lead to high rates of dynamic recovery and, hence, much lower rates of work hardening. For the  $45^\circ$  direction, in any deforming volume element, the two operating slip systems are co-planar and, thus, are not strong obstacles for each other. Hence, during the athermal hardening stage of deformation, there are virtually no statistical barriers to deformation generated for either active slip system. The major barriers to dislocation motion, in this case, can only be the geometrically necessary dislocation boundaries, formed to accommodate the shear strain incompatibility generated by only having the two slip systems active [4,8]. Thus, the athermal hardening rate is much lower for the  $45^\circ$  direction than for the  $0^\circ$  direction. On the other hand, with only co-planar slip systems active in the majority of the deforming volume element, there are no active cross-slip systems. The only areas where recovery would be occurring would be the regions containing the geometrically necessary boundaries, where a higher number of slip systems would be expected to be active. Consequently, a lower rate of recovery would be expected in the  $45^\circ$  direction compared to the  $0^\circ$  direction. In the case of the  $22^\circ$  direction, a somewhat similar behaviour to the  $45^\circ$  direction would be expected but with maybe slightly enhanced athermal hardening and dynamic recovery due to the greater number of active slip systems for each deforming volume element.

## 5. Conclusions

In the present work, an investigation of the tensile flow behaviour generated by a strong cube texture in aluminium alloy AA1050 at temperatures of 77 K and 298 K has been undertaken. At both temperatures, significant flow stress anisotropy was observed; however, the orientation variation of the flow stress with strain was a function of the testing temperature. Utilising texture analysis it was concluded, that under conditions of athermal hardening, the testing directions with multiple slip systems operative produced higher levels of work hardening. Conversely under dynamic recovery deformation conditions, these directions produced lower rates of hardening due to access to a greater number of cross-slip systems.

## References

- [1] G. Sachs: Z. VDI, 72 (1928), 734.
- [2] G.I. Taylor: J. Inst. Metals, 62 (1938), 307.
- [3] S.I. Wright and U.F. Kocks: *Preferred Orientation Package - Los Alamos, Manual*, July 1994 edition, Los Alamos National Laboratory, U.S.A. (1994).
- [4] F. Li and P.S. Bate: Acta Metall. Mater., 39 (1991), 2639.
- [5] B.P. Wynne: Ph.D. Thesis, Dept. of Materials Engineering, Monash University (1997).
- [6] H. Mecking: *Work Hardening in Tension and Fatigue*, ed. A.W. Thompson, AIME, 67 (1975).
- [7] J.F.W. Bishop and R. Hill: Philos. Mag., 42 (1951), 414.
- [8] P. Cizek, B.P. Wynne, Hong Lu and B.A. Parker: Mater. Sci. Eng. A, 219 (1996), 44.